

Recovering of local magnetic K-indices from global magnetic Kp-indices using neural networks: an application to Antarctica

Antoni Segarra^{*}, Juan José Curto

Observatori de l'Ebre (OE), CSIC - Universitat Ramon Llull, Roquetes, Spain

Article history

Received December 29, 2014; accepted June 30, 2015.

Subject classification:

K-index, Neural networks, Local magnetic indices, Antarctica.

ABSTRACT

This paper describes a method to obtain local magnetic index, K, from the global index, Kp. Until now, however, for the cases of areas without magnetic observatories, to estimate the geomagnetic activity there, global indices were the only option. The methodology that we used to estimate local index was based on neural networks. This tool has a great potential for processing information from complex systems as in the case of the geomagnetic system. Local K index calculated with this method resulted to be a better option than directly using the global index Kp when we need an indicator of geomagnetic activity in a specific area. The best results of our method were for moderate and high geomagnetic activity, which are of major interest in Space Weather.

1. Introduction

The magnetic variations on the magnetograms are different at each observatory. They mainly depend on the latitude of the observatory and the local time. We need a quantitative measure of the amount of magnetic disturbance at any time and, consequently, we need to introduce magnetic indices. These indices are often used as inputs of different regional models to describe the geomagnetic or ionospheric behavior [e.g., Zolesi and Cander 1998, Pietrella and Perrone 2008, Pietrella 2012]. There is a great variety of indices used to measuring the degree of magnetic disturbance for various purposes. In this paper, we will focus our attention in two indices: K-index (local) and Kp-index (planetary), which are widely used in geophysical studies.

The K-index is a local index. It was introduced by Bartels in 1939 [Bartels et al. 1939]. Each observatory assigns a digit ranging from 0 to 9 to both H and D, two components of the magnetic field, for every three-hour interval starting at midnight, universal time (UT). The digit is based on the range of the element during the three-hour interval normalized on a standard quasi-logarithmic scale [Mayaud 1980]. Several scales are applied, each one being specified by the amplitude, in nT, that

corresponds to K=9. Bartels chose the appropriate scale for each observatory, considering each one to have roughly the same frequency distribution of K-indices. The factors of proportionality between each scale were derived empirically for each observatory and reflect different geomagnetic effects depending on the observatory location. However, it was later shown that the “goal of proportional grids leading to similar significance of K values is achieved only in the subauroral regions, where the geomagnetic perturbations have similar local time and seasonal variations and where the distribution of K index is lognormal” [Menvielle and Berthelier 1991]. In order to derive this index, some caution is required when determining the three-hourly range on which the K-index is based, since what is wanted is not simply the range, but the range after the diurnal variation has been removed [Mayaud 1967]. K-indices have to measure the disturbance variations which are not related to the diurnal variation. As the diurnal variation differs from day to day, observers - in the case of hand-scaled - or algorithms - in the case of automatically - must exercise great care when estimating it [Menville et al. 1995]. In some situations, it is very difficult to obtain the diurnal variation, for instance in the recovery phase after magnetic storms which modify the baseline of the diurnal variations.

The other index that we take into consideration is the Kp-index, which is derived from the preceding one. Kp is a global index. It was introduced by Bartels in 1949 [Bartels 1949]. Kp involves a digit ranging from 0 to 9 with a subdivision in thirds (0, 0+, 1-, 1, 1+, ...) for each three-hour interval starting at midnight, UT. It is worked out from the K-index of a group of 13 observatories (11 in the Northern Hemisphere, mainly in North America and Western Europe, and only 2 in the Southern Hemisphere), this irregular distribution implies that Kp-index is biased due to Northern Hemi-

sphere. Kp-indices are meant to measure and compare different disturbances at different times. Bartels recognized that K indices from different observatories had to be “standardized” (Ks, s from standardized) before they could be combined into a planetary index. Bartels handled the latitudinal and local time/seasonal corrections. Both corrections had the same condition: K values must have the same frequency distribution. To obtain the Ks value, the latitudinal variation was corrected with the definition of K=9 scales for each observatory; and the local time/seasonal variation was corrected through conversion tables. In this way, each three-hour value from the group of 13 selected observatories was calculated on basis of latitude conversion table, K=9 scale, and after that, converted into Ks using the local time/seasonal conversion tables [Bartels 1949, 1951]. As a result of this process, each K measurement was transferred through statistical tables to a specific location, Niemegek, and to a specific time, autumn, in order to be compared under the same conditions. The Kp-index gives us information on global magnetic activity, but it is an abstract index which does not give specific information of the disturbance in a specific location at a specific time.

A significant problem related to magnetic indices is the irregular distribution of the observatories. Numerous in the Northern Hemisphere and very scarce in the Southern Hemisphere, these observatories, however, are the only source of local indices. The inverse process of obtaining local indices from global indices is our aim. It is not an easy task because there is not any relating algorithm. The process of constructing Kp-index implies a transformation of local K through statistical tables. Then, using selected observatories, an average of Ks is calculated and this gives the Kp. To obtain local indices from global indices at a specific place you need to have the statistical table for this place, and also be able to undo the calculation of the Ks average. The main problem to undo this process remains on the statistical tables; these tables are constructed to have the same frequency distribution of K for every observatory, and are significantly different for each observatory.

The observatories distribution over the world is very irregular. With the time, the number of observatories has increased, but, even now, there are still large areas without observatories. The aim of this work is making an assessment of the geomagnetic activity in remote areas which usually are poorly covered with observatories. Having an assessment about geomagnetic activity in areas without observatories would be helpful to have a complete view of geomagnetic activity in any part of the Earth. There are different ways to try to do this. When the K-value for an observatory is not available, the easiest method to obtain a good approxi-

mation is to use the K-values of the nearest observatory. However, we are interested in remote areas, with low number of observatories, and so, this method would not be suitable. A second method involves making an interpolation using other observatories, but, again, the reduced number of observatories and their irregular distribution in those remote areas also rule out the feasibility of this technique. Finally, a third method involves attempting to undo the process whereby the Kp has been calculated. In this way, we propose a method to obtain local assessment derived from a global index. We compute local index K from a global index, Kp, through neural networks.

The neural network models are known to have the property of learning from cases and with ability to handle complex nonlinear physical phenomena. This neural network capability in space weather, related to predictions, has been demonstrated in various studies [Uwamahoro et al. 2012, Watthanasangmechai et al. 2012]. In the field of geomagnetism, Segarra and Curto [2012] applied neural networks for sudden commencement automatic detection. Lundstedt and Wintoff [1994] used neural network to predict geomagnetic storms using solar wind data. Wu and Lundstedt [1996, 1997], Lundstedt et al. [2002] and Kugblenu et al. [1999] demonstrated the ability of neural network for Dst forecast. Takalo and Timonen [1997] used neural networks for AE-index forecasting. Duka and Hyka [2008] checked multiple neural networks to predict the evolution of the three components of the global geomagnetic field. Boberg et al. [2000] developed a method for the prediction Kp-index based on neural networks, other authors used different methodology with the same aim, for example Costello [1997] or Wing et al. [2005]. A few models have been developed for the prediction of the local K-index [Virjanen et al. 2008, Kutiev et al. 2009].

As a validation of our method, we compute K values for a specific and remote place, Livingston (LIV) ($62^{\circ}39'44''$ S, $60^{\circ}23'41''$ W geographic coordinates; $52^{\circ}50'13''$ S, $8^{\circ}57'42''$ E, geomagnetic coordinates). Livingston Observatory is an unattended observatory during the major part of the year, only there are staffs during summer season. There, when data are retrieved, local K indices are automatically calculated by the adaptive smoothing method recommended by INTERMAGNET [Novozynsky et al. 1991].

2. Methodology - Neural networks

Neural networks can be defined as a form of computation inspired in biological models. Their name comes from their similarity with the human brain in two aspects: the fact that knowledge is acquired by learning; and that links, which are connecting the neu-

rons, store the information using a weight function [Hopfield and Tank 1985].

Neural networks consist of elements (neurons) and connections (weight functions) that are adjusted, or trained, so that a particular input leads to a specific target output. These elements are inspired by biological nervous systems. As in the natural world, network behaviour is possible due to the connections existing between individual elements. A network requires two or more layers. Each layer consists of simple elements (neurons), with the ones in each layer connected to the neurons in the next layer through weighted links. The process of determining these weights is called “learning”. The first layer receives the external information; the last one produces the output or solution and the intermediate layers have no connection with the external “world”, so they are called hidden layers. A neural network can be trained to perform a particular function by adjusting the values of the weights. The weights are adjusted according to different rules for example back-propagation learning rule: a learning rule which weights and biases by error-derivative (delta) vectors back-propagated through the network.

Generally, in order to train neural networks, a particular input is introduced along with a target, which represents the desired output. The network begins to create different connections selecting those variables which may make the final output reach the desired target. When network training ends, the information has flowed through the network several times and the weights have been modified according to the accuracy of the output regarding the target.

2.1. Back-propagation

Neural networks, in particular a feedforward back-propagation network, are very efficient in the recognition of patterns or hidden structures in a dataset [Demuth and Beale 1994]. Feedforward neural network with error back-propagation is a method commonly used for mapping multivariable inputs to multivariable outputs [Rumelhart et al. 1986]. This kind of network extracts features from a data set and learns the associations between the inputs and the outputs. Input information crosses the network (forward), being transformed by the intermediate layers, and the obtained output is compared with the target. The difference or error is returned back to the network, crossing the network backwards [Rojas 1996]. Repeating this process adjusts the weights of the connections in the network to minimize the difference between the current and desired output of the net. There is no conclusive way to determine the appropriate number of layers and neurons. These figures are determined on a trial-and-error basis.

The amount of data and the distribution used to train the network is fundamental for an accurate determination of the network. For a successful manipulation, training data should include cases of every possible relevant option in the distribution [Kröse and Van der Smagt 1996]. Therefore, there is an aspect concerning the number of neurons in the hidden layer that should be emphasized: more neurons, which theoretically would entail a greater capacity of calculation, does not necessarily mean better results [Demuth and Beale 1994].

In order to find the appropriate network, two major selections should be considered [Nakamura et al. 2007]: the parameters of the physical problem to be resolved, which will determine the input information for the neural network, and the parameters of the neural network architecture. Furthermore, these choices have to be made in parallel.

2.2. Input parameters

In order to choose the input parameters, we need to consider the physics of the problem, which variables could affect the value of K-index. Depending on the locations of the observatories, different effects from the flowing currents around the magnetosphere are recorded. Thus the observatories located at night local time are more affected by the particles that came from the magnetotail, especially during substorm time [Parkinson 1983]. Thus, we take the geomagnetic latitude and geomagnetic longitude of each observatory as input variables. Diurnal and seasonal variations also contribute to modulate regular and irregular variations, the ionospheric current systems are modulated by thermal effects of the Sun and their incidence to the Earth, so ionospheric current systems have a seasonal dependence [Parkinson 1983]; consequently we also take the time and day of the year as input variables. And as our objective is transforming K_p-index to local index, we must take K_p-index as an input variable.

The neural network input “vector” for each observatory was determined as: geomagnetic latitude and longitude, time, day of the year and K_p-index. The neural network target is the corresponding K-index, but only for our training stations, as our test station, LIV, is excluded from the training set. The network found the relationship between these variables and the target.

We worked with the values of K obtained for the years 2003, 2004 and 2005 in the INTERMAGNET network (International Real-time Magnetic Observatory Network). We have data from 68, 72 and 78 observatories respectively according to their availability. In addition to that, we have the data from the station in Livingston (LIV) for the same period [Marsal et al. 2004, 2005], which is useful to test the results of our neural network.

2.3. Data sets

After defining the variables of physical interest we selected the observatories whose data we were going to use in order to train the neural network. We cannot directly include all the observatories because their irregular distribution around the Earth, and as we commented above, Kp-index is biased for Northern America and Western Europe observatories. If we take all observatories the results would be biased due to the overweight of the overpopulated areas. As our test station is Livingston, which is located in a very special region - the Antarctic region - we had to select our data set even more carefully.

To train the neural network we were faced with two possible options: either take observatories from all around the planet - although well distributed -, or just choose observatories close to Livingston. To sum up, we could either use a global data set network or a local data set one. We tried both options.

2.3.1. Global network

We need to attain a regular distribution of observatories, with special attention paid to the number of observatories in each hemisphere. Figure 1 shows the global distribution of the observatories included in the study.

We have 7 files containing the data of 6 observatories each, making 42 observatories in total. These files are intended to offer a regular distribution of observatories; two in the Northern Hemisphere, two in the Southern Hemisphere, and two near the Equator. Moreover, the training was carried out randomly, both in terms of which observatories were chosen for each group and also in which order those observatories were selected.

2.3.2. Local network

The other approach involves taking the local data set network with those observatories close to our test station, as shown in Figure 2. In this case we take all the observatories in the Southern Hemisphere, except those in the auroral zone because of their different magnetic behaviour. Livingston is an Antarctic observatory but it is considered as a mid-latitude station from the point of view of geomagnetism.

Unlike the global data set network, all the available observatories were included in this second approach. There are just 11 available stations out of the 42 stations selected for the global data set network. Livingston is not included in the training data set as we kept it apart for checking purposes.

2.4. Neural network parameters

The other elements to be chosen are the parameters of the neural network, such as the number of layers, the number of neurons in each layer, the transfer function included in the neurons, and the training algorithm. After running several tests to delimit our research, we concentrated on 2, 3 or 4 layers (counting the input, hidden and output layers), with a maximum of 40 neurons each. A higher number of neurons would involve more computing time but would not lead to a significant improvement in our results.

Due to the training method chosen, the neural network used the error back-propagation method, which means the weights keep adjusting as the information flows through the network. The transfer function was a log-sigmoid for the hidden layers and a linear function for the other layers. After running several

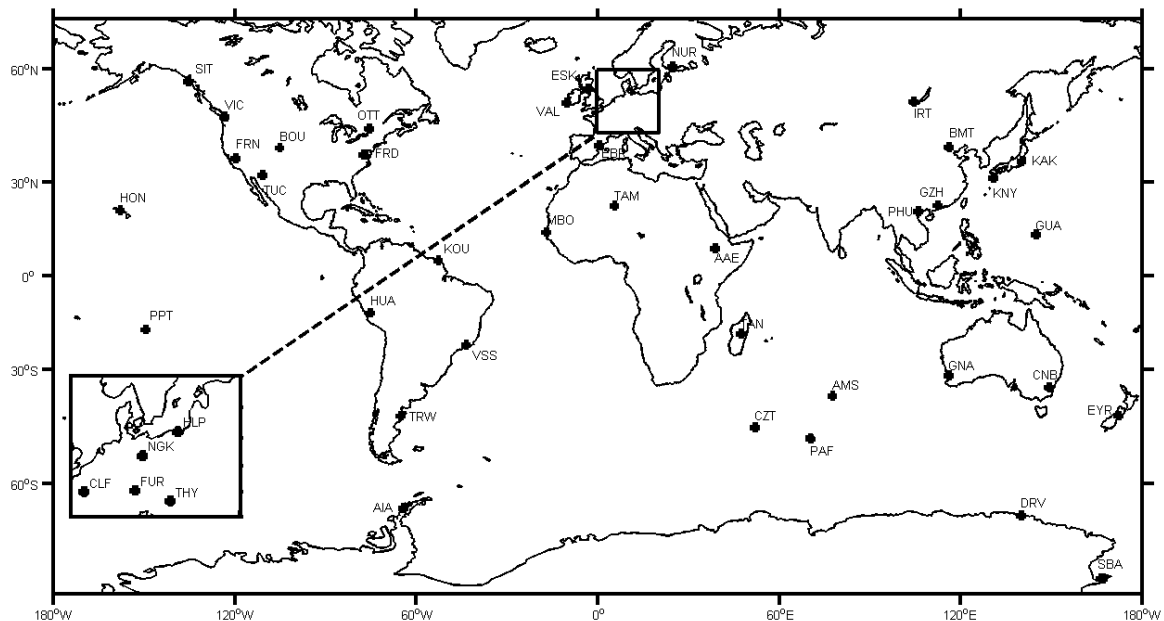


Figure 1. Global distribution of magnetic observatories used in the option one in the training process of the network.

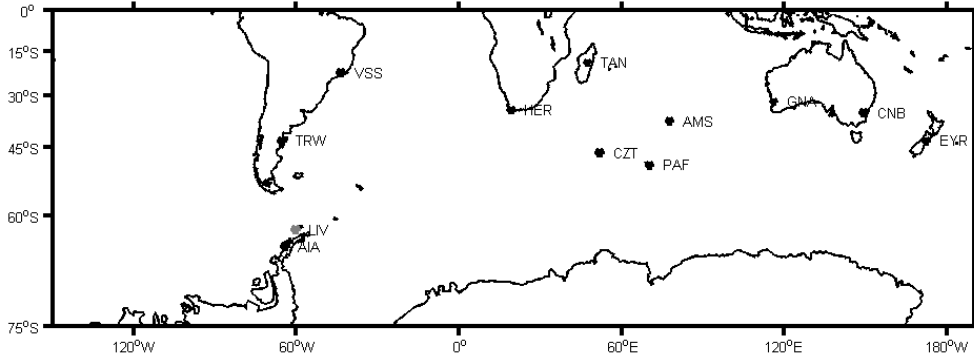


Figure 2. Local distribution of magnetic observatories in the neighbourhood of our test station, Livingston (LIV), used in the option two in the training process of the network.

tests, we chose these functions because they give us the best performance. The training method we used was a conjugate error gradient algorithm, based on the search of direction of the negative gradient. To accelerate the training process, we used the Powell-Beale condition [Demuth and Beale 1994]

$$|g_k^T - {}_1g_k| \geq 0.2 \|g_k\|^2 \quad (1)$$

where g_k is the current gradient, g_k^T its transposed matrix and ${}_1g_k$ is the gradient computed in the previous cycle. The search of the negative gradient is made along the conjugate gradient direction; the direction search is periodically reset to the negative of the gradient. This technique restarts if there is very little orthogonality left between the current gradient and the previous gradient. If this condition is satisfied, the direction search is reset to the negative of the gradient.

In order to choose between all the possible parameters of the neuronal network, we had to compare the results obtained in each case. We created and trained the neural network and then we compared the results obtained with the real data of the magnetic station of Livingston.

We ran a series of tests taking different numbers of layers and neurons per layer (the results are shown in Table 1). We were interested in finding a network able to produce an output Kn (n from network) with the high and low values of K.

After a series of tests, we decided to work with three different architectures: a two layer network, with 40 and 1 neuron per layer respectively; a three-layer network, with 20, 10 and 1 neurons per layer respectively; and a four layer network, with 40, 10, 10 and 1 neurons per layer respectively. We decided work with these three neural networks because these neural networks were able to provide almost the full range of the K values. Among the other options which were tested, the case of 4-layer network [40, 30, 20, 1] is worth mentioning: it provided values of Kn over 9, and thus it was discarded.

Next, with our chosen parameters, we needed to check which kind of data set network, either global or local, may lead to better results. We ran series of tests on the selected neural networks with a global and local data set network of observatories (Table 2). To decide which the best neural network for our aim is, we used the same criteria than above; we need a network able to produce low and high K values. We decided that the best neural network in our case is a three later network, with 20, 10 and 1 neuron per layer respectively.

In all three network architectures, using a global data set network of observatories, the networks pro-

| Number of layers | Neurons for layer | Kn range |
|------------------|-------------------|----------|
| 2 layers | [40 1] | 0-7 |
| | [20 1] | 1-5 |
| 3 layers | [40 20 1] | 0-7 |
| | [20 10 1] | 0-8 |
| | [10 5 1] | 0-5 |
| 4 layers | [40 30 20 1] | 0-13 |
| | [40 10 10 1] | 0-7 |
| | [20 10 5 1] | 0-6 |
| | [10 5 5 1] | 1-7 |

Table 1. Summary of the Kn range for each network parameter set.

| Data sets | NN architecture | Kn range |
|-----------|-----------------|----------|
| Global | [40 1] | 1-4 |
| | [20 10 1] | 1-6 |
| | [40 10 10 1] | 1-4 |
| Local | [40 1] | 0-7 |
| | [20 10 1] | 0-8 |
| | [40 10 10 1] | 0-7 |

Table 2. Summary of the Kn range depending on data set and neural network architecture.

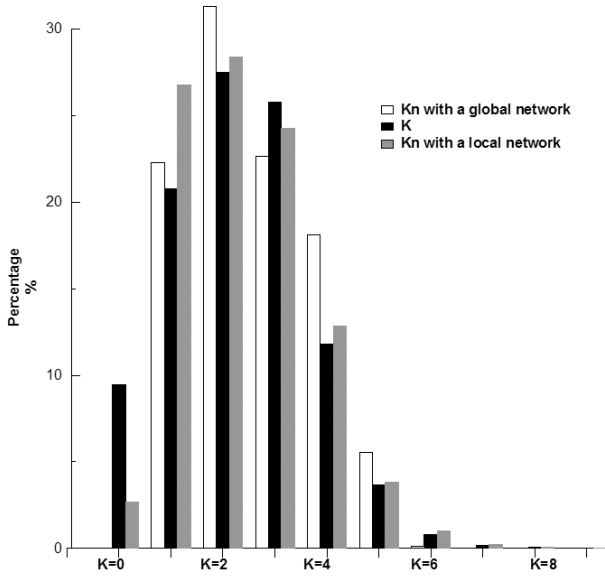


Figure 3. Comparison between the frequency distribution of K_n obtained through a local network (grey bar) and another K_n obtained with a global network (white bar), and also K real frequency distribution in LIV (black bar).

duce K but they do not cover all the range of possible values. However, the local data set network of observatories does. So the option that leads to the best results is a local network of observatories. This is because when training the neural network with observatories from different regions, the network is not able to recognize the different latitudinal effects that affects the magnetic signatures of the different observatories, and tries to produce an average. The neural network can not correct the latitudinal effects on the basis of the input parameters. But when training the network with

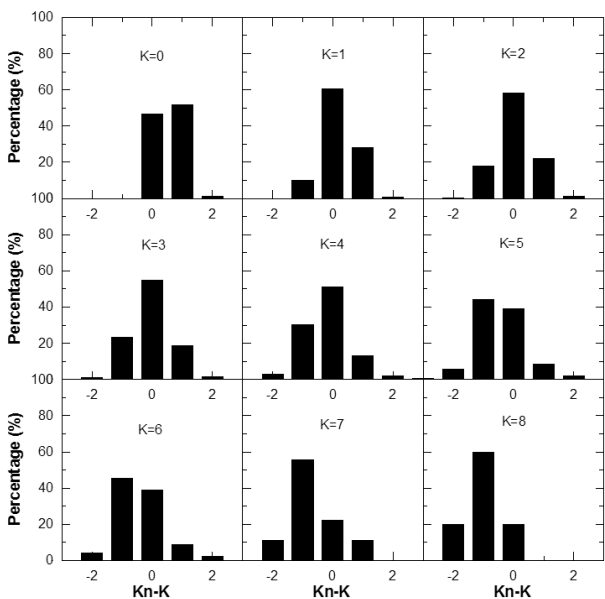


Figure 4. Histograms with the percentage of differences between K_n and K for each class of K -index.

observatories from the same region, they are subjected to the same magnetospheric effects, and the neural network is able to recognize these patterns, because we used time and day of the year as input parameters and the neural network can correct the local time/seasonal variations.

Nevertheless, we must also verify the frequency distribution obtained by the neural network, the percentage of each class that the network obtains. We understand by class the subset of three-hourly periods having the same degree of magnetic activity determined by the value of K . We must also verify whether a neural network works better for high or low K values. Figure 3 shows frequency distributions for a local data set network (grey bar), a global data set network (white bar), and the real frequency distribution of K at Livingston (black bar). We compare K_n obtained with a local data set network and K_n obtained with a global data set network. Clearly, the local data set network seems to be superior, especially for moderate K values.

Figure 3 illustrates another question: all these neural networks produce fewer $K_n=0$ than we expected. It seems that the neural network converts a significant number of $K_n=0$ into $K_n=1$. We detected this problem in a large variety of architectures of neural networks and with different data tests. On the basis of our empirical experience, we assume that the few number of $K_n=0$ is due to a systematic boundary problem of operational function of the selected network. The neural network gives us an integer number from 0 to 9, and if we do not apply this condition we can see that there is an important number of cases in which K_n is around 0.5-0.7. So, taking $K_n < 0.7$ as the $K=0$ value, we can adjust our results with more accuracy. All the figures and results which we show below were obtained using these criteria. At the highest boundary, $K=9$, we have another problem but from a different source. The neural network learns from cases but with three years of data only 0.6% of our training data set lies between $K=7$ to $K=9$. In this situation is remarkable that we have adequate predictions for these values.

3. Results

With the selected neural network, we represent the distribution of the differences between K_n and K that the neural network gives for each class of real K -index at the magnetic station of Livingston, Figure 4. In this figure, for low values of K , the differences between K_n and K are more than 90% centred around 0 and ± 1 . For K values greater than 5, the differences are biased to -1 value, with a ratio of more than 80% between 0 and ± 1 . In the strict sense, a good “hit” occurs when the difference between the K -computed by the network, K_n ,

and the K-real is zero. In order to determine if the results can be considered to be correct, we need to take into account that an error of ± 1 may be accepted. Such an error is “de facto” acceptable, mainly for low K values, since some uncertainty is involved in the determination of the K index mainly due to the problem in extracting the diurnal variation. A two-unit difference can already be considered problematic, and in the case of a three-unit difference, the error is unacceptable.

In order to see the advantages of using the K of the neural network instead of directly using Kp, we use the same kind of graphs, but now focusing on the differences between Kp and K-real at Livingston (Figure 5). For all K values the differences are centered around 0, but have a distribution similarly to distribution showed in Figure 4. To show the benefits to use Kn we have to compare the frequency distributions of Kp and Kn (Figure 6). We applied the same criteria used by Bartels et al. [1939] to establish the K=9 logarithmic scale for each observatory. We see that for low K values, the Kp distribution matches better than Kn to K values. For these ranges, when we have quiet solar conditions, this is especially significant because the diurnal variation is dominant in magnetograms, and this is usually the range with a greater error in the process of determining K. But for moderate and high magnetic activity (high K) - when the most important situations in Space Weather happen -, the Kn distribution is much better than the Kp distribution when we compare them to the local K.

On the basis of deviations between amplitudes in the frequency distribution, we can compare the differences between both distributions. If we take Kp as the

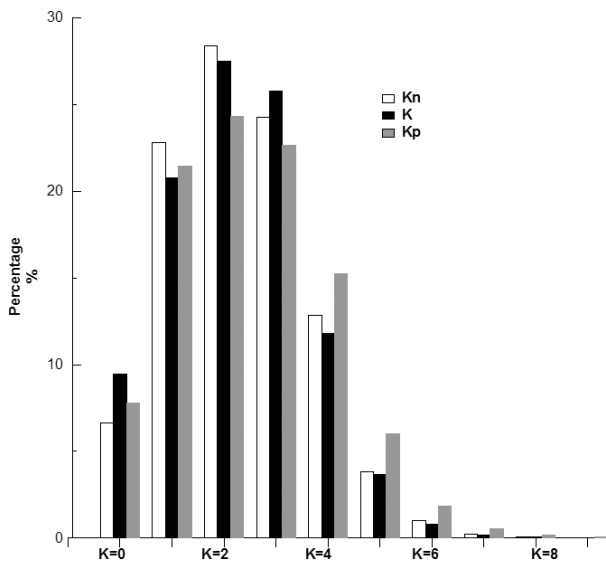


Figure 6. Comparison between the frequency distributions of K-real at Livingston (black bar), Kn calculated with the network (white bar) and Kp (grey bar).

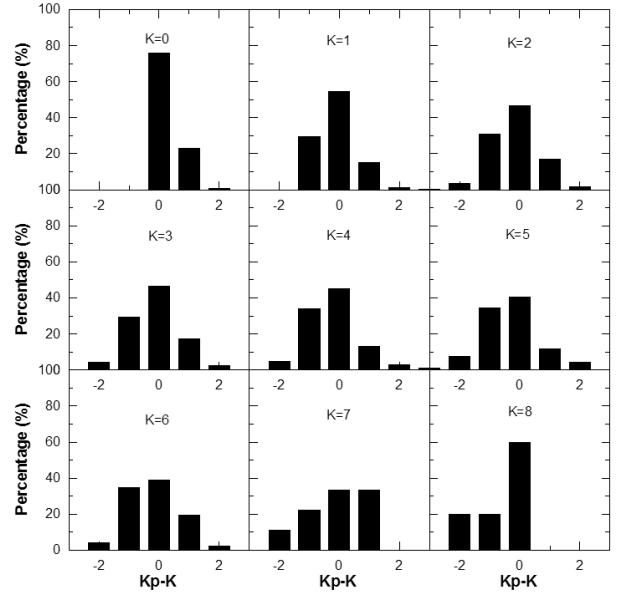


Figure 5. Histograms with the percentage of differences between Kp and K for each class of K-index.

K-local, the difference rate is 3% for K=1, 11% for K=2, and the rate increases considerably for higher values of K (29% and 64% for K=4 and 5). However, if we take Kn as the K-local, the difference rate is higher for low K (9.5% for K=1), but from K=2 upwards the difference lessens and keeps constant around 5% for K=2 to K=5.

To show the advantages of our method, in the Figure 7, we compare the frequency distributions of K values obtained with our method with those obtained with two different interpolation methods. We obtained K values for LIV interpolating the K values of observatories close to LIV. We checked two interpolating cases,

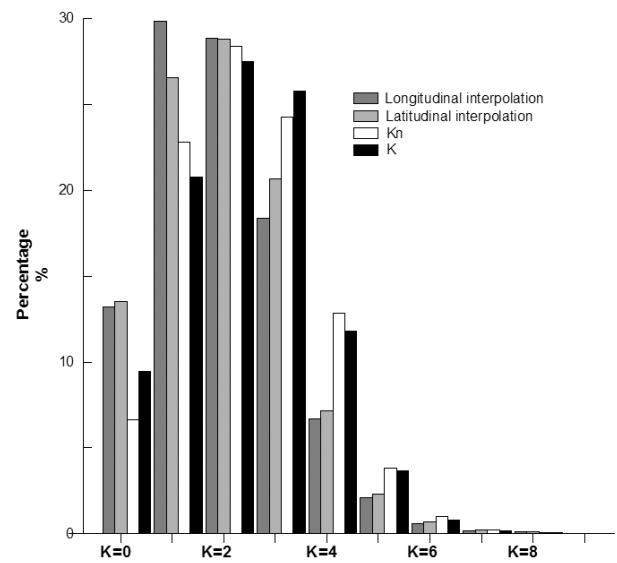


Figure 7. Comparison between the frequency distribution of the longitudinal interpolation results (dark grey bar), the latitudinal interpolation results (light grey bar), Kn calculated with the neural network (white bar) and the K-real at LIV (black bar).

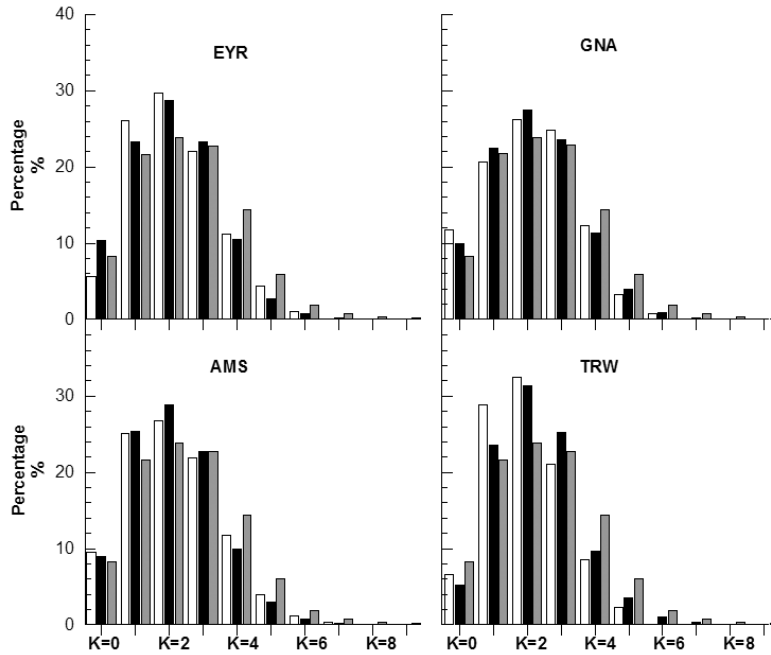


Figure 8. Comparison between the frequency distributions of K-real (black bar), Kn (white bar) and Kp (grey bar) for 4 observatories which are inside the influence zone of the network.

one derived from a latitudinal interpolation and the other one from a longitudinal interpolation. We obtained K values of LIV interpolating the K values of AIA and TRW observatories (light grey bar in Figure 7), located around similar longitude. The other interpolation method implies the observatories of TRW and CZT (dark grey bar in Figure 7), this two observatories are located around the same latitude. In the same figure, we plot the frequency distribution obtained by our method, Kn (white bar in Figure 7), and also the frequency distribution of the real K (black bar in Figure 7). For all K ranges the distribution of Kn match better the real values than the interpolation methods, specially for $K=1$, $K=3$ and $K=4$. This comparison reinforces the goodness of the results obtained by the neural network.

Until now, this computation was applied to the case of Livingston, and it is obvious that under conditions of disturbance, Kn is a better choice than Kp. At this point, it is worthy checking if the same neural network may be applied to other observatories in the same zone. Thus, we had to check if our neural network works correctly at other observatories in the Southern Hemisphere. We could not take another observatory for testing directly, because we had already used all the available observatories for training. So, first we had to remove the data of the observatory we were interested in from the training set, and then we trained the network again and checked the new results. In Figure 8, we represent the frequency distributions at 4 observatories, Eyrewell (EYR), Gngangara (GNA), Martin de Vivies-Amsterdam Island (AMS) and Trelew (TRW).

The network responds well enough for all these observatories, showing the same features than Livingston observatory. We can conclude that for the zone of middle latitudes in the South Hemisphere, taking the Kn calculated with the neural network is better than taking Kp directly, especially in periods of magnetic activity. As this zone is very under populated with observatories, this method could be very useful.

4. Conclusions

K index is one of the most popular geomagnetic activity indicators. The aim of this research was to estimate a more accurate local K-index which would be especially useful for remote zones with not available observatories. Our method adjusts the frequency distribution of local K better than when replacing the unknown local data with global indices Kp, especially under conditions of moderate and high magnetic activity, which are, by far, the most interesting conditions for the modellers of Space Weather.

We applied our method to the case of a remote observatory, Livingstone, as a test. We demonstrated that under disturbance conditions this method is a better choice than Kp. The same neural network is also able to produce appropriate values for a wide region under the same magnetic effects.

In the future, the network would be improved by being trained with more cases of very high K-indices ($K=8$ or $K=9$) taking advantage of years with high geomagnetic activity. Another interesting input variable to be considered might be the ordinal number of the year in the solar cycle or the Wolf number, which

would allow us to relate the value of the indices to the phase of the solar activity cycle.

These indices could be suitable to be introduced in regional models of Space Weather when local conditions are relevant because Kn are statistically more accurate than the direct use of Kp.

Acknowledgements. This research has been supported by Spanish government projects CTM2008-03033-E, CTM2009-13843-C02-01 and CTM2010-21312-C03-01 of MINECO. And also supported by project 2014 SGR 175 of Generalitat de Catalunya, and the project 2014-URL-Trac-039 of Ramon Llull University - Obra Social "la Caixa". The results presented in this paper rely on data collected at magnetic observatories. We thank the national institutes that support them and INTERMAGNET for promoting high standards of magnetic observatory practice (www.intermagnet.org).

References

- Bartels, J., N.H. Heck and H.F. Johnston (1939). The three-hour-range index measuring geomagnetic activity, *Terr. Magn. Atmos. Elec.*, 44, 455.
- Bartels, J. (1949). The standardized index, Ks, and the planetary index, Kp, *IATME Bull.*, 12b, 97, IUGG Pub. Office, Paris.
- Bartels, J. (1951). An attempt to standardize the daily international magnetic character figure, *IATME Bull.*, 12e, 109.
- Boberg, F., P. Wintoft and H. Lundstedt (2000). Real time Kp predictions from solar wind data using neural networks, *Phys. Chem. Earth*, 25 (4), 275-280.
- Costello, K.A. (1997). Moving the rice MSFM into a real-time forecast mode using solar wind driven forecast models, Ph.D. thesis, Rice University, Houston, Texas.
- Demuth, H., and M. Beale (1994). *Neural Network Toolbox for use with MATLAB*, The Mathworks Inc., Natick, MA, USA.
- Duka, B., and N. Hyka (2008). Using neural networks to study the geomagnetic field evolution, *Annals of Geophysics*, 5 (5/6), October/December, 755-767.
- Hopfield, J.J., and Q.W. Tank (1985). 'Neural' computation of decisions in optimization problems, *Biol. Cybern.*, 52, 141-152.
- Kröse, B., and P. Van der Smagt (1996). *An introduction to Neural Networks*, University of Amsterdam, Amsterdam.
- Kugblenu, S., S. Taguchi and T. Okuzawa (1999). Prediction of the geomagnetic storm associated Dst index using an artificial neural network algorithm, *Earth Planets Space*, 51, 307-313.
- Kutiev, I., P. Muhtarov, B. Andonov and R. Warant (2009). Hybrid model for nowcasting and forecasting the K index, *J. Atmos Solar-Terrestrial Phys.*, 71, 589-596.
- Lundstedt, H., and P. Wintoft (1994). Prediction of geomagnetic storms from solar wind data with the use of a neural network, *Annales Geophysicae*, 12, 19-24.
- Lundstedt, H., H. Gleisner and P. Wintoft (2002). Operational forecasts of the geomagnetic Dst index, *Geophys. Res. Lett.*, 29 (24), 2181; doi:10.1029/2002GL016151.
- Marsal, S., J.M. Torta, L. Gaya-Piqué, J.J. Curto, E. Sanchlement, J.G. Solé, D. Altadill, A. Ugalde, A. De Santis, E.M. Apostolov, L.F. Alberca and A. García (2004). Observaciones geomagnéticas de la Isla Livingston, Antártida 2003 y campaña 2003-2004, *Boletín del Observatorio del Ebro*, CD-ROM (ISSN 1579-4032), 121 pp.
- Marsal, S., J.M. Torta, L. Gaya-Piqué, J.J. Curto, E. Sanchlement, J.G. Solé, D. Altadill, A. Ugalde, A. De Santis, E.M. Apostolov, L.F. Alberca and A. García (2005). Observaciones geomagnéticas de la Isla Livingston, Antártida 2004 y campaña 2004-2005, *Boletín del Observatorio del Ebro*, ISSN 1885-9712.
- Mayaud, P.N. (1967). *Atlas des indices K*, IAGA Bull., 21, IUGG Publ. Office, Paris, 113 pp.
- Mayaud, P.N. (1980). *Derivation, Meaning, and Use of Geomagnetic Indices*, Geophysical monograph 22, American Geophysical Union, Washington D.C.
- Menvielle, M., and A. Berthelier (1991). The K-derived planetary indices: Description and availability. *Rev. Geophys.*, 29, 415-432.
- Menvielle, M., N. Papitashvili, L. Häkkinen and C. Sucksdorff (1995). Computer production of K indices: review and comparison of methods, *Geophys. J. Int.*, 123, 866-886.
- Nakamura, M.I., T. Maruyama and Y. Shidama (2007). Using a neural network to make operational forecasts of ionospheric variations and storms at Kokubunji, Japan, *Earth Planets Space*, 59, 1231-1239.
- Novozyński, K., T. Ernst and J. Jankowski (1991). Adaptive smoothing method for computer derivation of K-indices, *Geophys. J. Int.*, 104, 85-93.
- Parkinson, W.D. (1983). *Introduction to Geomagnetism*, Scottish Academy Press, Edinburgh.
- Pietrella, M., and L. Perrone (2008). A local ionospheric model for forecasting the critical frequency of the F2 layer during disturbed geomagnetic and ionospheric conditions, *Annales Geophysicae*, 26, 323-334.
- Pietrella, M. (2012). A short-term ionospheric forecasting empirical regional model (IFERM) to predict the critical frequency of the F2 layer during moderate, disturbed, and very disturbed geomagnetic conditions over the European area, *Annales Geophysicae*, 30, 343-355; doi:10.5194/angeo-30-343-2012.
- Rojas, R. (1996). *Neural Networks - A Systematic Introduction*, § 7: The backpropagation algorithm,

- Springer-Verlag, Berlin.
- Rumelhart, D.E., G.E. Hinton and R.J. Williams (1986). Learning representation by back-propagating errors, *Nature*, 323, 533-536.
- Segarra, A., and J.J. Curto (2012). Automatic detection of sudden commencements using neural networks, *Earth Planets Space*, 65, 791-797.
- Takalo, J., and J. Timonen (1997). Neural network prediction of AE data, *Geophys. Res. Lett.*, 24 (19), 2403-2406.
- Uwamahoro, J., L.A. McKinnell and J.B. Habarulema (2012). Estimating the geoeffectiveness of halo CMEs from associated solar and interplanetary parameters using neural networks, *Annales Geophysicae*, 30, 963-972.
- Virjanen, A., A. Pulkkinen and R. Pirjola (2008). Predictions of the geomagnetic K index based on its previous value, *Geophysica*, 44 (1-2), 3-13.
- Watthanasangmechai, K., P. Supnithi, S. Lerkvaranyu, T. Tsugawa, T. Nagatsuma and T. Maruyama (2012). TEC prediction with neural network for equatorial latitude station in Thailand, *Earth Planets Space*, 64, 473-483.
- Wing, S., J.R. Johnson, J. Jen, C.-I. Meng, D.G. Sibeck, K. Bechtold, J. Freeman, K. Costello, M. Balikhin and K. Takahashi (2005). Kp forecast models, *J. Geophys. Res.*, 110 (A04203); doi:10.1029/2004JA010500.
- Wu, J.G., and H. Lundstedt (1996). Prediction of geomagnetic storms from solar wind data using Elman recurrent networks, *Geophys. Res. Lett.*, 23, 319-322.
- Wu, J.G., and H. Lundstedt (1997). Neural network modeling of solar wind-magnetosphere interaction, *J. Geophys. Res.*, 102 (A7), 457-466.
- Zolesi, B., and L.R. Cander (1998). Advances in regional ionospheric mapping over Europe, *Annali di Geofisica*, 41 (5/6), 827-842.

Corresponding author: Antoni Segarra,
Observatori de l'Ebre (OE), CSIC - Universitat Ramon Llull,
Roquetes, Spain; email: asegarra@obsebre.es.